Early Stages of Flame Dynamics in Tubes and Mechanism of Tulip Flame Formation

Michael A. Liberman[1], Chengeng Qian[2], Cheng Wang[2]

[1]Nordita, KTH Royal Institute of Technology and Stockholm University, Hannes Alfvéns väg 12, 114 21 Stockholm, Sweden. [2]State Key Laboratory of Explosion Science and Technology, Beijing Institute of Technology, Beijing, 100081, China

1   Introduction

Dynamics of a flame in tubes is the basis for understanding the characteristics of combustion processes under confinement. The phenomenon of tulip flame, which is the inversion of the flame front from convex in the direction of flame propagation to a concave shape with a cusp pointing towards the burned gas, has been known for almost a century, and after its first observation by Ellis [1] it was studied by many authors experimentally and using numerical simulation. However, despite a large number of experimental, theoretical and numerical studies, there is still no unambiguous explanation of the physical mechanism responsible for the tulip flame formation, see e.g. [2, 3]. The proposed mechanisms of the tulip flame formation are still controversial and not entirely clear. Of particular note is the study by Guénoche [4], who hypothesized that rarefaction waves generated by a decelerating flame are a key factor in the tulip flame formation.

In this paper, the dynamics of a flame ignited near the closed end of a tube and propagating to the opposite closed or open end is studied by solving the fully compressible reactive Navier-Stokes equations. It is shown that the tulip flame formation is a pure hydrodynamical phenomenon in agreement with recent experimental studies [3]. The inversion occurs due to rarefaction waves produced by the decelerating flame when its surface decreases due to quenching of the rear parts of the flame skirt at the side walls.

2   Earlier stages of flame dynamics in a tube with no-slip walls

Before the development of the tulip flame shape, different stages of flame propagation can be distinguished. After the flame ignition at the closed end of the tube, the flame front quickly acquires a nearly hemispherical shape. Clanet and Searby [15] have shown that the next stage is the formation of the finger shape flame, with the flame tip X_{tip} accelerating as $X_{tip} \propto exp(4\Theta U_f t / D)$, where D is the tube diameter (width in the 2D case), $\Theta = \rho_u / \rho_b$ is the ratio of the densities of unburned and burned gases, and U_f is the laminar flame velocity. This stage lasts a short time $t \approx D / 2\Theta U_f$ and it ends when the rear edge of the flame skirt touches the sidewalls.

The expansion of the high temperature burned products between the flame and the closed end of the tube pushes the unburned gas towards the opposite end of the tube, thus creating an upstream flow ahead of the flame. Because of the wall friction the velocity in the upstream flow is maximal at the tube axis and drops to zero at the tube walls in the boundary layer of thickness δ_l. The inhomogeneous flow stretches the flame so that different parts of the flame front move at different speeds, and the flame front takes a shape similar to the velocity profile in the flow ahead of the flame. The flame sheet "repeats" to some extent the shape of the velocity profile in the upstream flow, remaining almost flat in the bulk with the trailing edges of the flame skirt extending backward in the boundary layer along the sidewalls. Every point at the flame front moves relative to the unreacted mixture with velocity U_f and simultaneously it is carried by the upstream flow with its local velocity $u_u^+(x,y)$ immediately ahead of this point. In the laboratory reference frame, the local velocity of the flame front at the point (x,y) is $U_{fl}(x,y) = U_f + u_u^+(x,y)$. The stretched flame consumes fresh fuel over a larger surface area, which results in an increase in the rate of heat release per unit projected flame area. The increase in the rate of heat release results in a higher volumetric burning rate, and a higher effective burning velocity based on the average heat release rate per frontal area of the flame sheet. A higher burning velocity leads to an increase of the flow velocity ahead of the flame, which in turn leads to an increase in the flame front stretching. Thus, a positive feedback coupling is established between the upstream flow and the combustion wave velocity. With accuracy $\delta_l / D << 1$ the flame surface grows linearly in in time, which leads to an exponential increase of the flame velocity $U_{fL} \propto exp(\alpha \Theta U_f t / D)$, where α is a dimensionless coefficient of the order of unity [5]. After the rear edges of the flame skirt touched the sidewalls, the flame skirt begins to stretch along the sidewalls, the angle between the flame skirt and the sidewall decreases, and the rear part of the flame skirt becomes almost parallel to the sidewalls. Shortly thereafter, this part of the flame skirt touches the sidewalls and extinguished, which leads to a sharp reduction of the flame surface area and as a consequence, to sharp decrease in the average speed of the combustion wave. The decelerating flame begins to generate rarefaction waves, which reduce the flow velocity in the unburned mixture, and therefore the flame velocity. The reduced velocity of the flow ahead of the flame leads to an increase in the width of the boundary layer and a corresponding change in the velocity profile ahead of the flame, which will determine the shape of the inverted flame front. The thickness of a laminar boundary layer in the flow ahead of the flame is $\delta_l \approx 5X / \sqrt{Re}$, where $Re \approx u_u X / \nu \approx X(\Theta - 1)U_f / \nu$ is the Reynolds number, X is the coordinate along the tube. The mass of the unburned mixture passing through the tube cross-section is the same, but the thickness of the boundary layer increases with X. The Poiseuille flow with a parabolic velocity profile is formed when the boundary layer thickness becomes equal to half of the tube width. An estimate of the distance and the time that the flame travels before establishing a parabolic velocity profile is: $X_P \sim \Theta U_f D^2 / 100\nu$ and $t_P \approx D^2 / 104\nu$ [5]. For example, in a hydrogen/air mixture the Poiseuille flow in the tube of width 1cm establishes after a rather long time $\approx 50ms$ compared to the characteristic times of the flame front inversion or the transition to detonation $\approx 1-2ms$. On the contrary, in narrow channels ($D \leq 1mm$) a parabolic velocity profile establishes at the very early stage of the flame propagation, the flame accelerates without deceleration stage, and this is the reason why a tulip flame in narrow tubes has never been observed experimentally.

3   Numerical simulations of the tulip flame formation

The computations solved the multidimensional, time-dependent, reactive compressible Navier-Stokes equations including molecular diffusion, thermal conduction, viscosity and chemical kinetics. The 2D direct numerical simulations were performed using the DNS solver, which used the fifth order weighted

essentially non-oscillatory (WENO) finite difference schemes [6] to resolve the convection terms of the governing equations. A high-resolution simulation was used with minimum grid size, $dx \leq 20\mu m$, corresponding to 16 computational cells over the flame width. Since the tulip flame formation is expected according to experiments [3] to be a purely gas-dynamical process, a one-step Arrhenius chemical model was used in simulations, which were then compared with the results obtained in simulations with a detailed chemical model for hydrogen/air [7].

The numerical simulations of the stoichiometric premixed hydrogen/air flame were performed for a tube with both closed ends, with the tube width 0.6cm and the length 8.4cm. The flame was ignited near the left closed end and propagates to the opposite closed end. The parameters of the one-step chemical model for a hydrogen/air flame were taken the same as in [8]. Figure 1 shows the calculated time evolution of the flame surface area (length) F_f, the average combustion wave speed S_f, the local speed of the flame front at the channel axis $U_{fl}(x,0)$, and at the line $y=0.16cm$, where the tulip petal is formed, during the tulip shape formation.
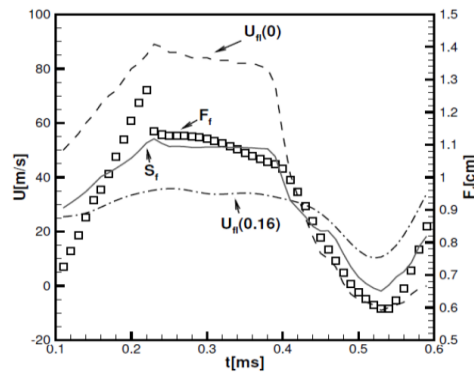
Figure 1: Time evolution of combustion wave velocity S_f, local x-component of the flame front velocities $U_{fl}(y=0)$ and $U_{fl}(y=0.16cm)$, and the flame surface area (length) F_f.

After 0.42ms, the average flame speed becomes equal to the speed of the flame front at $y=0.16cm$, which means that the flame front has become almost flat, and after 0.44ms, the speed of the center of the flame front becomes less than the speed of the flame front near the wall, and the flame front begins to invert. Figure 2 shows the velocity profiles in the unburned gas, $U_+ = u_u(X_{f+},Y_f)$, immediately ahead of the flame (left) and velocities of different parts of the flame front at selected times.
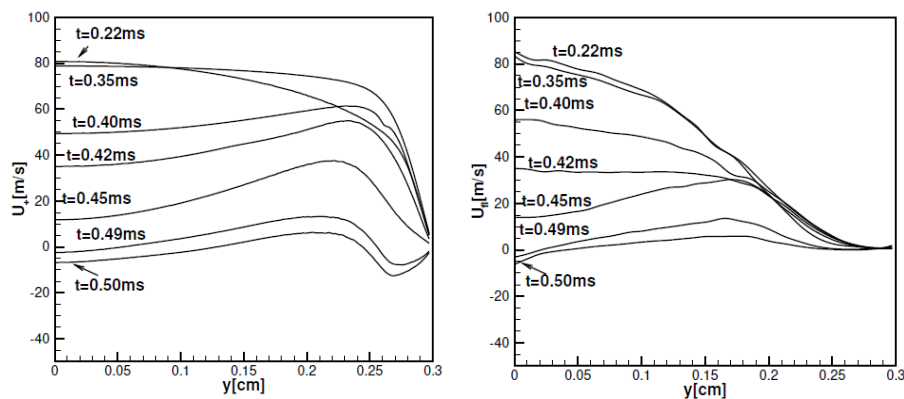
Figure 2: Velocity profiles ahead of the flame (left) and profiles of the velocity of the flame front.

It can be seen that rarefaction waves decrease the flow velocity ahead of the flame much stronger near the center line, and in this particular case they ultimately create a reverse flow, as it is shown in Fig. 3, which shows the calculated schlieren images and streamlines during the tulip flame formation.
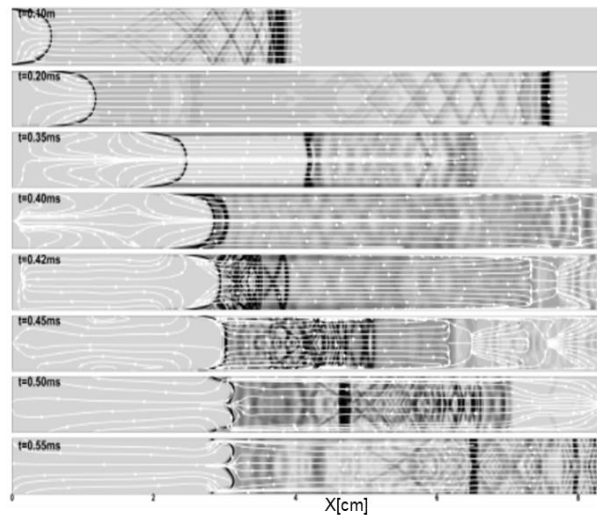
Figure 3: Sequences of calculated schlieren images and streamlines during the tulip flame formation

Figure 4 shows the evolution of rarefaction and pressure waves during the acceleration and deceleration phase, when the tulip flame is formed, as well as the change in the flow velocity along the centerline of the tube in the unburned gas ahead of the flame and into the burned gas behind the flame.
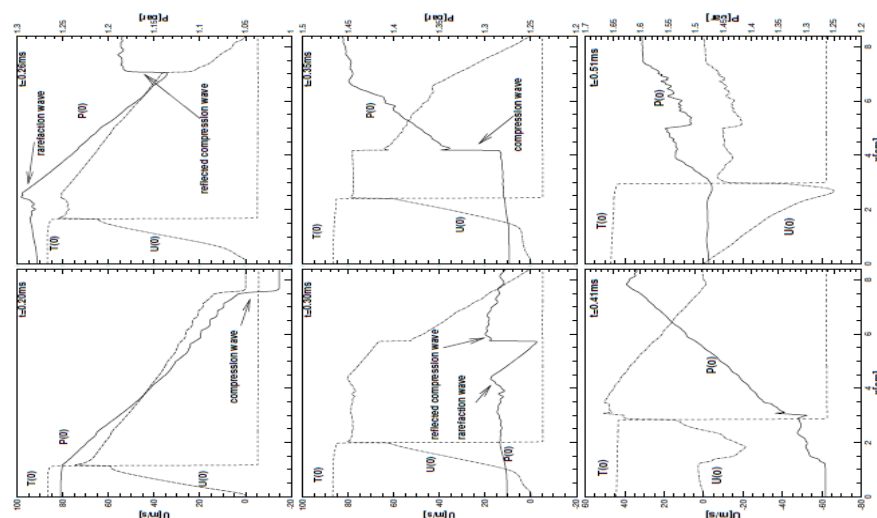
Figure 4: Pressure (solid line), temperature (dashed line) and flow velocity (dashed dotted lines) profiles at the tube axis during the tulip flame formation in hydrogen/air mixture.

Scenario of the tulip flame formation in the case of a hydrogen/air flame ignited at the tube axis near the closed end and propagating to the opposite open end is analogous to the case of a slow flame in a tube with both closed ends or a "fast" flame in a long tube. As an example, the formation of a tulip flame was simulated for the slowly reactive methane-air mixture in a tube with both closed ends and the same width and length as in figures 1-4. In simulations was used a one-step Arrhenius model for a methane/air flame with parameters as in [41] with the laminar methane/air flame velocity $U_f = 0.38 m/s$. Fig. 5 shows the evolution of the flame surface area, the average combustion wave velocity, and the local velocities

of the flame front at the center line and close to the sidewall at $y=0.16cm$, where the tulip petal is formed. The left figure is for methane/air flame in a tube with both closed ends, and the right figure is for a hydrogen/air flame propagating to the opposite open end.
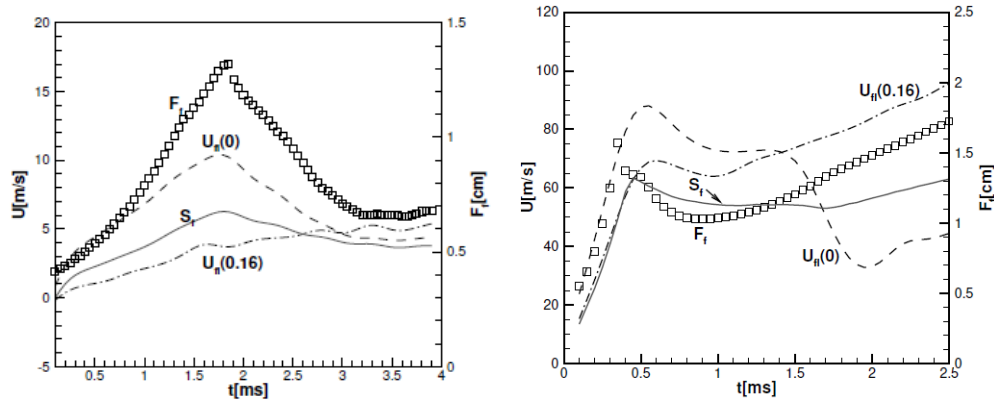
Figure 5: The evolution of the flame surface area, the average combustion wave velocity and velocities of the flame front at the lines $y=0$ and $y=0.16cm$. Left: methane/air flame in the tube with both closed ends, right: hydrogen/air flame propagating from the closed to the open end.

It is seen that the decrease in the surface are of the methane/air flame occurs more slowly than in the case of the hydrogen/air flame, due to the low velocity of the methane/air flame. Consequently, the intensity of rarefaction waves is lower, and the inversion of the flame front from a convex to a concave shape takes a longer time.

To verify how the choice of chemical model affects tulip flame formation, modelling of tulip flame formation using the Arrhenius one-step chemical model was compared to modelling using a detailed chemical model.
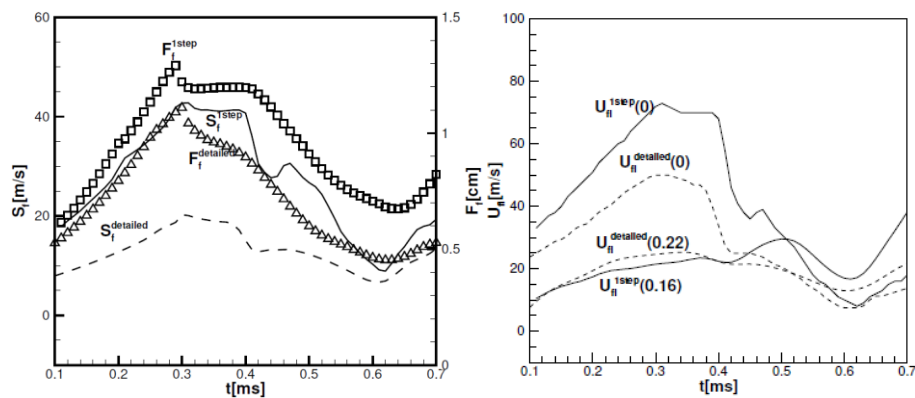
Figure 6: The evolution of the flame surface area, the average combustion wave velocity and velocities of the flame front at the central line and near the sidewall for simulations with one-step and with detailed chemical models.

It can be seen that in general, the dynamics and trend is the same in both cases one-step and detailed chemical models, including the time of the flame front inversion, which confirms that the tulip flame formation is a purely gas-dynamic process. However, there is some differences in the flow structures, which is seen in schlieren images in Fig. 7. Apparently, the differences are due to the different transport models in the case of a one-step chemistry and many species in the case of detailed chemical model.
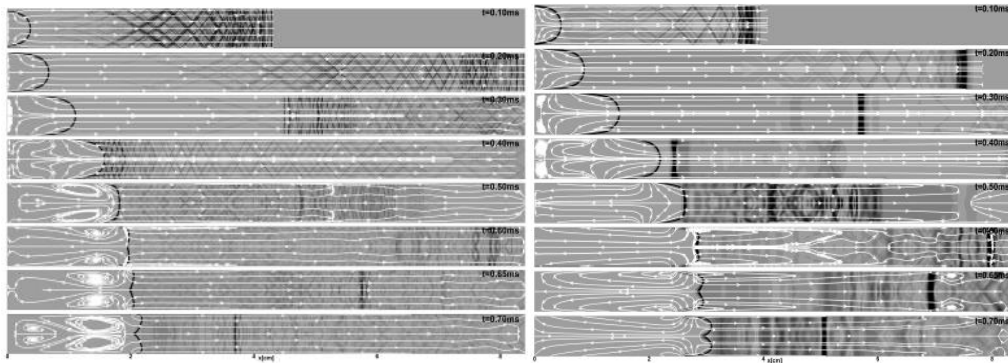
Figure 7: Sequences of calculated schlieren images and streamlines during the tulip flame formation

4 Conclusions

The numerical simulations provided details of flame dynamics and the processes through which the flame front inversion occurs from a convex shape with the cusp pointed in the unburned gas to a concave shape with a cusp pointing towards the burned gas. The simulations support the hypothesis proposed by Guenoche [4] that the initiation of tulip flame occurred due to rarefaction waves generated by the flame after the flame underwent a sudden deceleration associated with and the decrease of the flame surface area due to quenching of the rear part of the flame on the sidewalls. The simulations also confirm the conclusion observed from the experimental studies of the tulip flame formation [1] that the formation of a tulip flame is a purely gas-dynamic process, which does not involve the intrinsic flame instabilities.

References

[1] Ellis O. (1928). Flame movement in gaseous explosive mixtures. Fuel Sci.7: 502.

[2] Dunn-Rankin D. (2009). Tulip flames—the shape of deflagrations in closed tubes. In Combustion Phenomena: Selected Mechanisms of Flame Formation, Propagation and Extinction. Ed. J. Jarosinski and B. Veyssiere. CRC Press, Boca Raton (ISBN 978-0-8493-8408-0).

[3] B. Ponizy B, Claverie A, Veyssière B. (2014). Tulip flame - the mechanism of flame front inversion, Combust. Flame, 161: 3051.

[4] Guénoche H. (1964). Flame Propagation in Tubes and Closed Vessels. In: Non-steady Flame Propagation, G. H. Markstein ed. AGARDograph, Elsevier, 75: 107(ISBN 9781483196596).

[5] Liberman MA, Ivanov MF, Kiverin AD, Kuznetsov MS, Chukalovsky AA, RakhimovaTV. (2010). Deflagration-to-detonation transition in highly reactive combustible mixtures, Acta Astr., 67: 688.

[6] Guang-Shan Jiang, Chi-Wang Shu. (1996). Efficient implementation of weighted eno schemes. J. Comput. Physics, 126: 202.

[7] Kéromnès A, Metcalfe WK, Heufer KA, et al. (2013). An experimental and detailed chemical kinetic modeling study of hydrogen and syngas mixture oxidation at elevated pressures. Combust. Flame, 160: 995.

[8] Gamezo VN, Ogawa T, Oran ES. (2007). Numerical simulations of flame propagation and DDT in obstructed channels filled with hydrogen–air mixture. Proc. Combust. Inst. 31: 2463.

[9] Kessler DA, Gamezo VN, Oran ES. (2010). Simulations of flame acceleration and deflagration-to-detonation transitions in methane–air systems. Combust. Flame, 157: 2063.